**SANDIA REPORT**
SAND2020-2802
Printed March 2020

Sandia National Laboratories

# Evaluation of Multi-cell Failure Propagation

Joshua Lamb
Loraine Torres-Castro
June Stanley
Christopher Grosso
Lucas Gray

Prepared by
Sandia National Laboratories
Albuquerque, New Mexico
87185 and Livermore,
California 94550

Issued by Sandia National Laboratories, operated for the United States Department of Energy by National Technology & Engineering Solutions of Sandia, LLC.



Available to DOE and DOE contractors from
U.S. Department of Energy
Office of Scientific and Technical Information
P.O. Box 62
Oak Ridge, TN 37831

| | |
|---|---|
| Telephone: | (865) 576-8401 |
| Facsimile: | (865) 576-5728 |
| E-Mail: | reports@osti.gov |
| Online ordering: | http://www.osti.gov/scitech |

Available to the public from
U.S. Department of Commerce
National Technical Information Service
5301 Shawnee Rd
Alexandria, VA 22312

| | |
|---|---|
| Telephone: | (800) 553-6847 |
| Facsimile: | (703) 605-6900 |
| E-Mail: | orders@ntis.gov |
| Online order: | https://classic.ntis.gov/help/order-methods/ |

## ABSTRACT

Failure propagation testing is of increasing interest to the designers and end users of battery systems. One of the chief difficulties, however, is choosing an appropriate initiation method to perform the test. Single cell abuse testing is typically used to initiate thermal runaway but this can involve a large amount of additional energy injected into the system. It is assumed that this will have some impact on the behavior of a propagating thermal runaway event, but there is little data available as to how significant this would be. Further, it is ultimately difficult to develop viable propagation tests for compliance and public safety activities without better knowledge of how test methods will impact the results. This work looks at propagating battery failure with a variety of chemistries, formats, configurations and initiation methods to determine the level of significance of the chosen initiation method on the test results. We have ultimately found while there is some impact on the detailed results of propagation testing, in most cases other factors, particularly the energy density of the system play a much greater role in the likelihood of a propagation event consuming an entire battery. We have also provided some guidelines for test design to support best practices in testing.

# ACKNOWLEDGEMENTS

This work was funded by the United States Department of Transportation – National Highway Traffic Safety Administration. We would like to thank Dr. Abhijit Sengupta, Steven Summers and Phillip Gorney for their support and contributions to this effort.

## CONTENTS



## LIST OF FIGURES

## LIST OF TABLES

This page left blank

# ACRONYMS AND DEFINITIONS

| Abbreviation | Definition |
|---|---|
| Ah | Ampere-hour |
| COTS | Commercial off the shelf |
| LCO | Lithium cobalt oxide-graphite battery chemistry |
| LFP | Lithium iron phosphate-graphite battery chemistry |
| NMC | Nickel Manganese Cobalt – graphite battery chemistry |
| SOC | State of charge |

# 1. INTRODUCTION

Studies on the safety of lithium ion batteries (LIB) have long focused on the impact and aftermath of the field failure of a single cell. This has been driven by the fact that LIB have traditionally been used for small devices where 1) failure of a single cell would have little impact beyond the device and its user, and 2) the battery is unlikely to see a truly abusive condition under normal use. As LIB are considered for larger systems, including vehicle electrification and electric grid applications such as energy storage and smart grid applications, the impact of the failure of single cells and small groups of cells must be reexamined. Recent incidents have seen thermal events that have eventually consumed entire battery systems, stemming from myriad initial causes including mechanical intrusion [1], overheating [2] and overvoltage/overcharging. [3] Not only are the causes of failure becoming more diverse, but the impact of these failures is increasing as well. However, few systemic studies have been performed to determine how a localized thermal runaway event may impact a battery system as a whole, regardless of the initial mode of failure.

The thermal runaway behavior of single lithium ion cells is well studied. [4-16] Typical responses include venting of battery gasses, ejection of cell contents, extreme temperatures and in some cases self-ignition of the cell or ejected battery materials. It is less well known how these behaviors may impact a larger, more complex system. The failure of a single cell taken on its own may have little impact on the safety or performance of an electric vehicle system; however, the thermal and electrical impact on other cells in the system may be sufficient to cause a cascading runaway effect. In this scenario, the energetic thermal runaway of a single cell provides enough heat to neighboring cells within the battery to initiate thermal runaway. This can potentially lead to a chain reaction of failures which continues to propagate until the entire battery pack has been consumed by the thermal runaway . This worst-case scenario would result in a catastrophic release of energy within the confines of an electric vehicle, causing significant damage and presenting a potentially dangerous situation for the operator. Spotnitz et al. [16] introduced a model for emulating thermal runaway propagation in a battery pack. Their work proposed that the likelihood of full battery pack failure was influenced by several factors, including the abuse response of individual cells and the overall insulation of the battery pack. Particularly important is the thermal contact with other cells, and it was predicted that cells directly neighboring multiple other cells were more likely to cause a propagation through a battery pack.

The electrical configuration of cells may impact how failure propagates as well. Offer et al. [17] showed that even under normal conditions, varying resistances of connections between cells within a battery module may impact the local temperature of each cell. It is common practice to use blocking and discharge diodes within large parallel battery packs to prevent self-discharge of the battery through a shorted cell. [18] However, the thermal isolation between cells is often limited. Prismatic and pouch cells are often packed together either face to face or separated by thin plates used for active cooling. [19] Even if they are thermally isolated the electrical connections themselves have been shown to provide a path for heat transfer between cells. [13]

Work exploring the behavior of battery systems has largely been focused on long-term performance issues; [17, 19-24] however some information on failure propagation may be inferred. Much of the current handling of cell faults in battery packs involves the diagnosis and electrical handling of faulty cells within a system. Various methods exist for the detection of faulty cells [21]. Kim et al. [20] described a method for electrically isolating faulty cells from the battery pack. The science of fault detection is still in its infancy, and the most reliable indicators of battery health are still voltage and temperature monitoring of cells. Unfortunately, when considering battery safety, changes in cell voltage or temperature are only symptoms of a different issue and are not indicators of a root cause. These indicators often lag a root cause, and by the time a significant temperature increase or voltage change is observed the cell is undergoing a thermal runaway event that is too late to arrest.

Sandia National Laboratories has previously released details on failure propagation testing using nail penetration methods. [25, 26] This was chosen due to the very low energy imparted to the pack needed to induce failure. However, this may not always be realistic for every testing organization or laboratory. Other test methods studied have included single cell overcharge, single cell thermal ramp, high intensity light and laser based initiation. These all impart varying amounts of energy as estimated in Table 1.

**Table 1 Example of energies needed to initiate thermal runaway on a 3 Ah LCO pouch cell**

| Test | Energy Source | Conditions | Estimated Energy |
|---|---|---|---|
| 20 Pulse laser | IR Laser | 20 1.9 J pulses | 38 J |
| Nail Penetration | Mechanical | 20 mm penetration ~200 lb peak load | 1.8 J |
| Undirected light | Quartz lamp | Exposure to light source through aperture | 6000 J[1] |
| Thermal Ramp | Thermal | Heat to 200 °C | 6300 J[2] |
| Overcharge | Electrical | 1C to 200% SOC | 43200 J[3] |

An example of previous work performed at SNL is shown in Figure 1 and has explored failure propagation in small packs of cells. This work has predominantly focused on using nail penetration failure as the initiation method, as this has a low energy input into the cell and can in most cases produce a thermal runaway event in these configurations. However, this leaves little information on how changes to the initiation method chosen when designing propagation experiments might impact the behavior of the battery pack. The work presented in this report explores various conventional abuse methods as initiation methods for failure propagation tests and observes changes in the results.

[1] Based on radiometer measured flux through aperture.
[2] Calculated for hypothetical 40g cell – larger cells will require more energy.
[3] Calculated for a hypothetical overcharge at 3 A and 4 V on a 3 Ah cell.

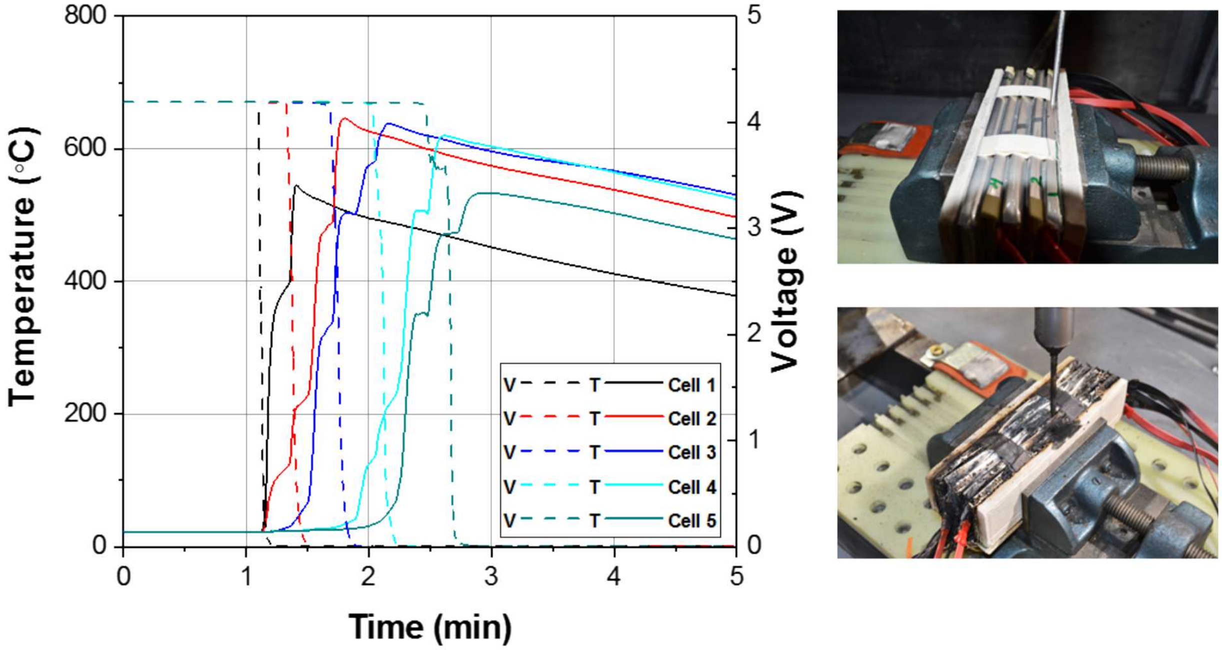


**Figure 1 Failure propagation on 5 cell pack of $LiCoO_2$-graphite cells initiated through single cell nail penetration**

## 2. TESTING PROCEDURES

Three primary cell types were tested as part of this effort. These cells were chosen to cover both cylindrical and pouch formats, as well as three chemistries with varied failure response. These cells were built into 10 cell packs in the case of cylindrical formats, and 7 cell packs in the case of pouch cell formats. The three cells targeted are 1) a 3.6 Ah high energy density NMC cell, 2) a 1.5 Ah commercial-off-the-shelf (COTS) 18650 format LCO cell, and a 3.2 Ah COTS 26650 format LFP cell. These can also be grouped roughly as a high, medium and low energy density cell, respectively. Figure 2 gives an overview of the cells tested as part of this work.

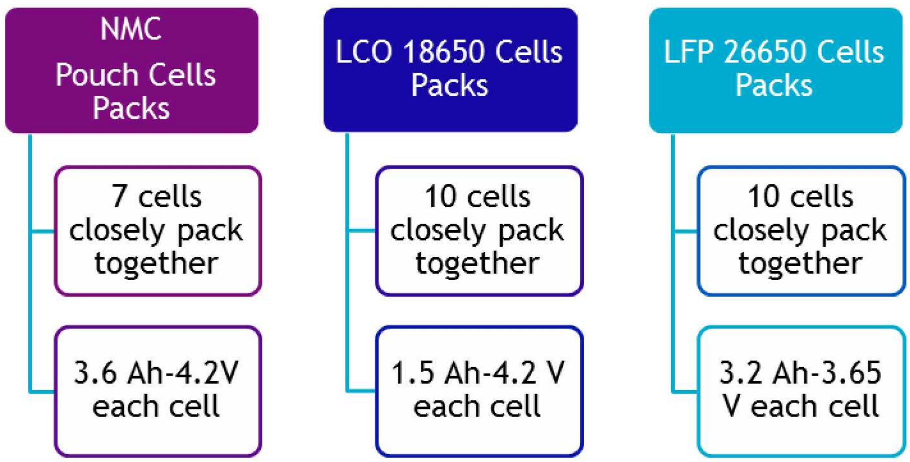


**Figure 2 Major cell packs tested for this work along with the generalized pack design used for thermal propagation testing. All cells are generally electrically isolated unless otherwise noted.**

The cells were arranged in the highest energy density packs possible for the format. Pouch cells were placed in a stack of cells with the central cell targeted for failure. Cylindrical cells were arranged in a close packed configuration with again the cylindrical cell targeted for failure. The general layout as well as measurement locations for thermocouples are detailed in Figure 3 and Figure 4.

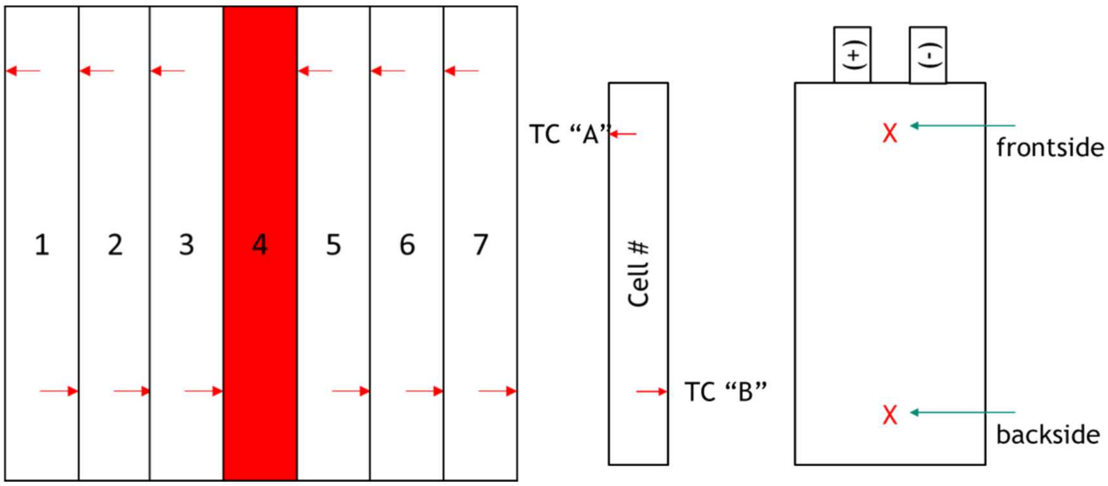


**Figure 3 Layout of pouch cell packs with single cell failure target highlighted in red and thermocouple locations noted.**

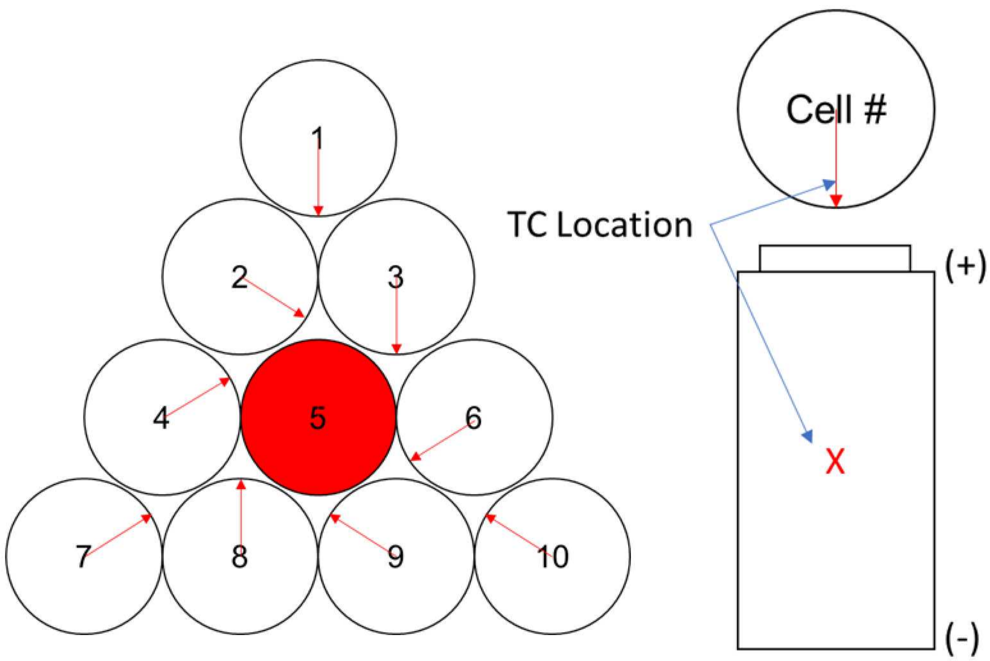


**Figure 4 Layout of cylindrical packs with single cell failure target highlighted in red and thermocouple locations noted.**

Single cell failure initiation was primarily performed by single cell overcharge, thermal ramp and nail penetration of the targeted cell. Overcharge testing is performed at a 1C nominal rate until cell failure is reached. A general voltage limit of 20 V is also used. The power supplies used will in most cases apply a constant 1C nominal current unless the cell reaches 20V. At this point the supplies will moderate the current to not exceed the limit voltage.

Thermal ramp was applied by attaching low profile heaters to the surface of the targeted cell. The targeted cell was then heated at a rate of 5 °C/minute until single cell failure was observed. This slower rate is used to ensure a bulk heating of the cell. Some limited testing using higher heating rates (at effectively the maximum rate of the heaters used) was performed to provide a comparison. The external heating was then stopped and any failure propagation allowed to progress until all energetic events had concluded.

Nail penetration was applied using a sharp conductive nail inserted into the cell. A 3 mm diameter nail was used for all tests and inserted at a rate of 1 mm/second until single cell failure was observed or the entire length of the nail was inserted (~50 mm). Single cell failure was defined as a thermal runaway event or an observed voltage loss of at least 100 mV. Once the failure ocurred, the behavior of the cell was observed and recorded until the cell was either fully consumed by thermal runaway or all energetic events had ended.

Limited testing was also performed by initiating failure with a small area, low profile heater applying heat to the target cell at a high rate. Small heaters of 1" square size were built by encapsulating nichrome heater wire in kapton tape. Heat was then applied at the maximum sustainable power (up to 200 W) for the heater until single cell failure was observed. Beyond these changes, these tests were handled in a similar manner to the thermal ramp test.

# 3. RESULTS AND DISCUSSION

## 3.1. Testing overview

Testing yielded generally mixed results in terms of the impact of the initiation method on the result. These results are summarized in Table 2-Table 4. The tables include, for each configuration and initiation method, the propagating failure type, with a full propagation indicating a thermal runaway that consumes the entire pack, a partial propagation indicating one or more cells beyond the target cell having exhibited some degree of failure, and no propagation indicating no severe damage observed to any cell beyond the initiating cell. The propagation time column, gives the time of the observed propagation event beginning with the initial thermal runaway and ending with the final failure event.

The overviews generally show that the high energy density NMC pouch cell pack reliably propagated after a single cell runaway was observed, with all cases fully consuming the pack within 60-80 seconds. Some variation was seen in the detailed results which are covered in the relevant sections below, but the propagation reliably occurred in all cases where single cell thermal runaway occurred. Even reducing the total stored energy did not top propagation, although it could increase the overall time to total failure.

The low energy density packs tested, the 26650 LFP packs, on the other hand had reliably limited thermal runaway response with no thermal runaway propagation observed in all cases. Even when adding a fully parallel connection, a propagation event generally wasn't observed.

The greatest impact of initiation method was observed in the pack with moderate energy density, the 10 cell LCO 18650 configuration. These results, summarized in Table 2 show either no or partial propagation when there are no electrical interconnects or other potentially exacerbating factors about the cell design. However, when adding parallel electrical connections to the cell, a full pack propagation was observed when using a thermal ramp initiation, while only a partial propagation was observed when using a nail penetration initiation.

**Table 2 Summarized results for NMC pouch cell packs.**

| **NMC Pouch Cells Packs: Part I** | | | |
|---|---|---|---|
| *Pack Configuration* | *Initiation Method* | *Propagation (Full, Partial, No)* | *Propagation time (s)* |
| • 7 cells<br>• 100% SOC<br>• No electrical connections | Thermal | • 1st test – Full<br>• 2nd test – Full | • 1st test – 65 s<br>• 2nd test – 77 s |
| • 7 cells<br>• 100% SOC<br>• No electrical connections | Electrical | • 1C OC - No<br>• 2C OC - Full | • 1st test – N/A<br>• 2nd test – 75 s |
| • 7 cells<br>• 100% SOC<br>• No electrical connections | Mechanical | • 1st test – Full<br>• 2nd test - Full | • 1st test – 84 s<br>• 2nd test – 79 s |
| **NMC Pouch Cells Packs: Part II** | | | |
| *Pack Configuration* | *Initiation Method* | *Propagation (Full, Partial, No)* | *Propagation time (s)* |
| • 7 cells<br>• 80% SOC<br>• No electrical connections | Thermal | • 1st test – Full | • 1st test – 64 s |
| • 7 cells<br>• 80% SOC<br>• No electrical connections | Mechanical | • 1st test – Full | • 1st test – 198 s |

**Table 3 Summarized results for LCO 18650 packs.**

| **LCO 18650 Cells Pack: Part I** | | | |
|---|---|---|---|
| *Pack Configuration* | *Initiation Method* | *Propagation (Full, Partial, No)* | *Propagation time (s)* |
| • 10 cells<br>• 100% SOC<br>• No electrical connections | Thermal | • 1st test – No<br>• 2nd test – Partial to two adjacent cells | • 1st test – N/A<br>• 2nd test – 414 s |
| • 10 cells<br>• 100% SOC<br>• No electrical connections | Electrical | • 1C OC - No | • 1st test – N/A |
| • 10 cells<br>• 100% SOC<br>• No electrical connections | Mechanical | • 1st test – No<br>• 2nd test - No | • 1st test – N/A<br>• 2nd test – N/A |
| **LCO 18650 Cells Pack: Part II** | | | |
| *Pack Configuration* | *Initiation Method* | *Propagation (Full, Partial, No)* | *Propagation time (s)* |
| • 10 cells<br>• 100% SOC<br>• 1S10P configuration | Thermal | • 1st test – Full<br>• 2nd test - Full | • 1st test – 522 s<br>• 2nd test – 393 s |
| • 10 cells<br>• 100% SOC<br>• 1S10P configuration | Mechanical | • 1st test – Partial<br>• 2nd test – Partial | • 1st test – Undetermined<br>• 2nd test – Undetermined |

**Table 4 Summarized results for LFP 26650 packs.**

| **LFP 26650 Cells Pack: Part I** | | | |
|---|---|---|---|
| *Pack Configuration* | *Initiation Method* | *Propagation (Full, Partial, No)* | *Propagation time (s)* |
| • 10 cells<br>• 100% SOC<br>• No electrical connections | Thermal | • 1st test – No<br>• 2nd test – No | • 1st test – N/A<br>• 2nd test – N/A |
| • 10 cells<br>• 100% SOC<br>• No electrical connections | Electrical | • 1C OC - No | • 1st test – N/A |
| • 10 cells<br>• 100% SOC<br>• No electrical connections | Mechanical | • 1st test – No<br>• 2nd test - No | • 1st test – N/A<br>• 2nd test – N/A |
| **LFP 26650 Cells Pack: Part II** | | | |
| *Pack Configuration* | *Initiation Method* | *Propagation (Full, Partial, No)* | *Propagation time (s)* |
| • 10 cells<br>• 100% SOC<br>• 1S10P configuration | Thermal | • 1st test – No<br>• 2nd test - No | • 1st test – N/A<br>• 2nd test – N/A |
| • 10 cells<br>• 100% SOC<br>• 1S10P configuration | Mechanical | • 1st test – No<br>• 2nd test – No | • 1st test – N/A<br>• 2nd test – N/A |

## 3.2. Impact of initiation methods in a low energy density pack

Nail penetration and thermal ramp tests were evaluated in the 10 cell LFP 26650 pack. An initial overcharge evaluation was performed, however it was quickly established that the cells were protected by a current interrupt device (CID) that blocked current flow early in testing and prevented using overcharge for propagation behavior analysis. Neither condition created a thermal runaway event severe enough to lead to a full cell runaway. However, some differences were observed in the detailed results.

The thermal ramp initiation (Figure 5 and Table 5) led to both a higher peak observed temperature after cell failure and higher observed temperatures in other cells in the pack. This demonstrates the impact on the initial conditions that thermal ramp testing creates. The bulk heating of a single cell ultimately leads to significant temperature rise in neighboring cells, with some cells ultimately reaching as high as 145 °C during the thermal ramp test. However, the energy released during the thermal runaway of the cell is not significant enough to lead to a thermal runaway propagation.

The nail penetration failure (Figure 6 and Table 6) meanwhile showed limited temperature increase, with no observed temperatures above 79 °C. The largest contributor to this difference is likely simply the elevated temperature at which failure occurred in the thermal ramp test. The failure under thermal ramp wasn't observed until 250 °C and also significantly elevated the temperature of neighboring cells. Ultimately, however, the limited energy available for thermal runaway along with the weaker thermal and geometric inefficiency of a cylindrical pack prevented enough energy being transferred to other cells to induce a propagating thermal runaway beyond the target cell.

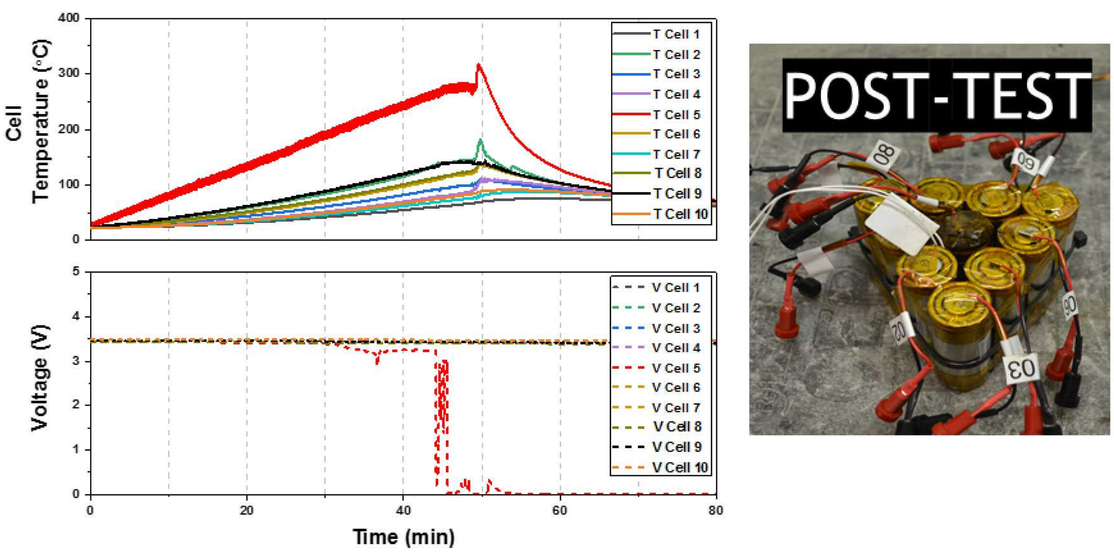


**Figure 5 Thermal ramp initiation in a 10 cell 26650 LFP pack**

**Table 5 Numeric results of data in Figure 5**

| **Test #1** | | |
|---|---|---|
| *Cell #* | *Max T (°C)* | *Max dT/dt (°C/min)* |
| 1 | 76 | 5 |

| | | |
|---|---|---|
| 2 | 182 | 120 |
| 3 | 110 | 68 |
| 4 | 112 | 84 |
| **5** | **317** | **347** |
| 6 | 135 | 54 |
| 7 | 88 | 47 |
| 8 | 140 | 59 |
| 9 | 146 | 89 |
| 10 | 91 | 11 |

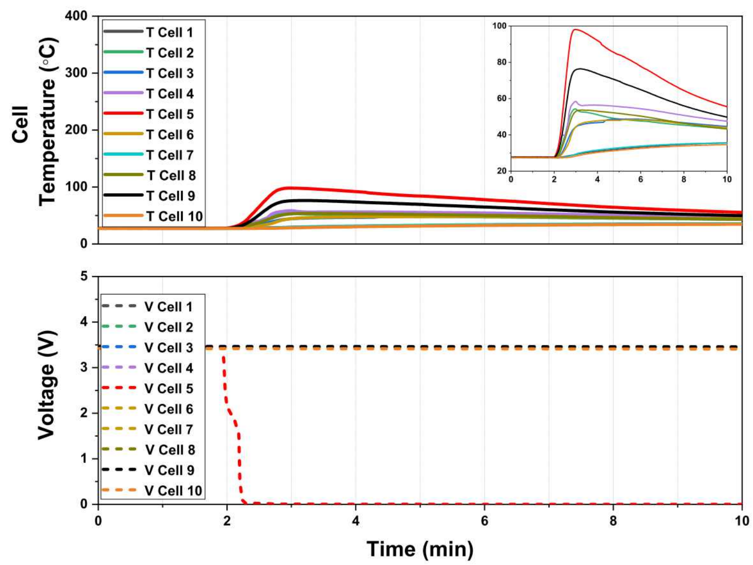


**Figure 6 Nail penetration initiation in a 26650 LFP pack.**

**Table 6 Numeric results from data in Figure 6**

| **Test #1** | | |
|---|---|---|
| *Cell #* | *Max T (°C)* | *Max dT/dt (°C/min)* |
| 1 | 28 | 7 |

| | | |
|---|---|---|
| 2 | 34 | 14 |
| 3 | 51 | 182 |
| 4 | 34 | 20 |
| **5** | **79** | **101** |
| 6 | 52 | 336 |
| 7 | 32 | 18 |
| 8 | 45 | 42 |
| 9 | 79 | 99 |
| 10 | 29 | 8 |

### 3.3. Impact of Initiation Method in a High Energy Density Pack

7 cell packs built with NMC pouch cells were initiated using nail penetration, overcharge and thermal ramp initiations with results shown in Figure 7. This represents the highest energy density pack tested, using both a high energy density NMC cell along with the efficient packing of multiple cells afforded by the pouch cell format. This led to a pack where thermal runaway easily propagated from cell to cell. At first glance, there are only nominal differences between each test method. The thermal runway propagated through the entire pack in all cases within 70-90 seconds of the initial failure.

Some variations were observed in detailed analysis of the results. Figure 7 and Table 7 show the results from thermal runaway initiation. The initial thermal runaway was observed after 33 minutes, but voltage loss was observed in the target cell at 31.5 minutes. The target cell also had the highest observed temperature at 629 °C. All heating rates observed were relatively similar.

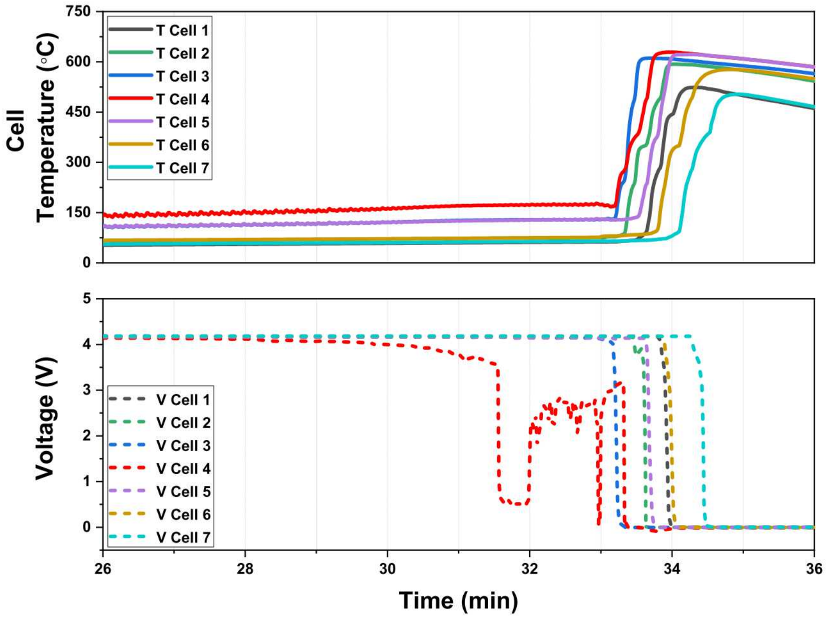


**Figure 7 Thermal runaway propagation initiated in a 7 cell NMC pack using single cell thermal runaway.**

**Table 7 Numeric data of results in Figure 7.**

| **Test #1** | | | | |
|---|---|---|---|---|
| *Cell-runaway order* | *Propagation time (s)* | *Onset T (°C)* | *Max T (°C)* | *Max dT/dt (°C/min)* |
| 3 | 0 | 133 | 611 | 2517 |
| **4** | **9** | **170** | **629** | **1488** |
| 2 | 17 | 87 | 593 | 1523 |
| 5 | 28 | 141 | 622 | 1520 |
| 1 | 39 | 90 | 524 | 1756 |
| 6 | 43 | 95 | 577 | 1496 |
| 7 | 65 | 94 | 503 | 1539 |

Overcharge testing seen in Figure 8 shows a very high rate failure of the target cell, which also reaches a temperature of 713 °C. However, compared to the thermal ramp, the heating of the remainder of the pack was significantly limited, so that only the nearest neighbors to the target cell showed a significant rise in temperature above ambient prior to onset of thermal runaway. Therefore, while the total time to consume the pack was similar, this created a situation where there were easily observable time gaps between sets of cells going into runaway. Ultimately, the overcharge test created a single cell runaway that was measurably more severe than the thermal ramp runaway, but the neighboring cells were less impacted by the lead up to failure. It is worth noting that overall this is a significant injection of total energy into the pack, effectively doubling the energy of a single cell within the pack.

The behavior of the peak temperatures is also worth commentary. During thermal ramp testing, all peak temperatures (with the exception of the outer cells) were fairly close to each other. Meanwhile the overcharge test results showed peak temperatures were lower for cells that were farther removed from the initial failure location. This indicates some possibility that overcharge and thermal ramp may have some different observable impacts if testing very large systems.

Results using single cell nail penetration are shown in Figure 9. This data shows a peak temperature that is slightly lower than that observed during thermal ramp or overcharge tests, with a peak observed temperature of 549 °C. All cells were also at ambient temperature when the initial failure occurred. This has the lowest energy injection into the pack of the cells tested, yet the high energy density of the pack ensures that full propagation occurs in this case. This suggests that the elevated temperatures seen in the center of the pack during overcharge testing are more a function of the large amount of energy forced into the failed cell, causing a more energetic thermal runaway of that cell than occurs through a temperature driven thermal runaway event.

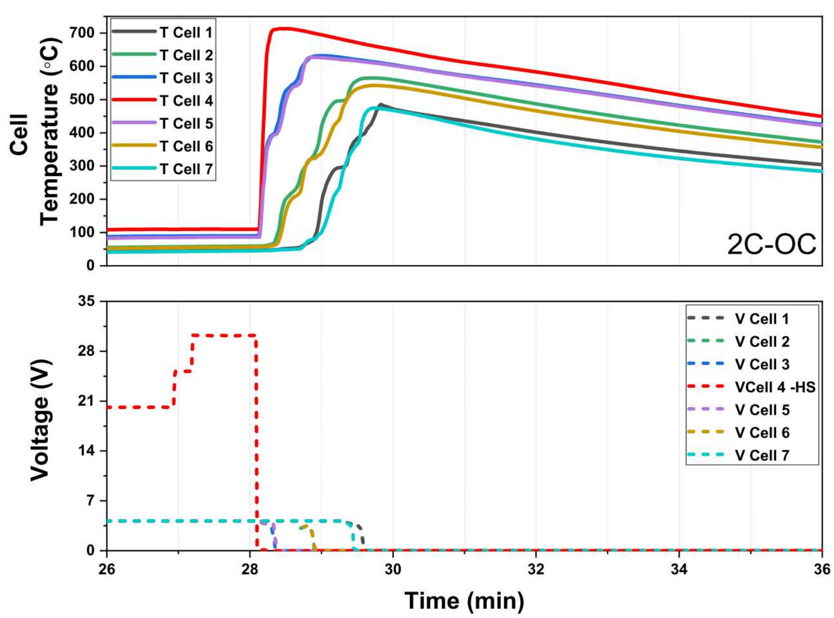


**Figure 8 Thermal runaway propagation in a 7 cell NMC pack initiated using a single cell 2C overcharge**

**Table 8 Numeric data of results in Figure 8**

| **Test #2** | | | | |
|---|---|---|---|---|
| *Cell-runaway order* | *Propagation time (s)* | *Onset T (°C)* | *Max T (°C)* | *Max dT/dt (°C/min)* |
| **4** | **0** | **110** | **713** | **5789** |
| 3 | 2 | 90 | 632 | 2920 |
| 5 | 4 | 115 | 627 | 2888 |
| 2 | 32 | 226 | 565 | 1179 |
| 6 | 36 | 216 | 542 | 1076 |
| 7 | 69 | 229 | 474 | 1100 |
| 1 | 75 | 305 | 486 | 1354 |

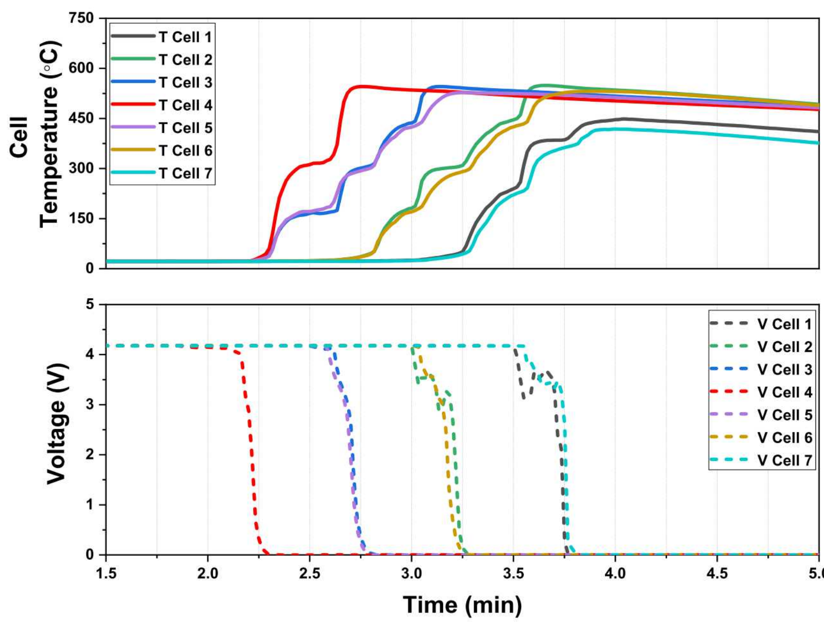


**Figure 9 Thermal runaway propagation of 7 cell NMC pack initiated using single cell nail penetration**

Table 9 Numeric data of results shown in Figure 9

| **Test #1** | | | | |
|---|---|---|---|---|
| *Cell-runaway order* | *Propagation time (s)* | *Onset T (°C)* | *Max T (°C)* | *Max dT/dt (°C/min)* |
| **4** | **0** | **RT** | **546** | **2741** |
| 5 | 26 | 184 | 528 | 1429 |
| 3 | 28 | 171 | 546 | 1734 |
| 2 | 51 | 181 | 549 | 1515 |
| 6 | 53 | 180 | 531 | 1051 |
| 1 | 81 | 240 | 448 | 1833 |
| 7 | 84 | 233 | 418 | 1362 |

## 3.4. Impact of initiation method under moderate energy densities

Single cell thermal runaway and nail penetration were used as initiation methods in a 10 cell pack built with 18650 format lithium cobalt oxide-graphite (LCO) cells, with results shown in Figures 10 and 11, and documented in Tables 10 and 11. This pack configuration represents a moderate energy density configuration, with a high energy density chemistry with well-established catastrophic thermal runaway results, offset by the lower packing efficiency of cylindrical cells. Overcharge initiation was also briefly explored, however, it proved impossible to trigger a single cell thermal runaway due to the use of CID in cylindrical cells. A brief overview of results shows that this configuration produces some variance between the initiation methods used, with thermal ramp leading to two additional cells failing in the pack while no propagation occurs during nail penetration.

Further examination of the data shows that the excess heating of surrounding cells during the thermal ramp test is the likely culprit of this variance. Several cells near the target are at 150 °C or higher at the time the target cell goes into thermal runaway. The elevated temperature of the target cell at the onset of thermal runaway also leads to a significantly higher temperature in the target, with the thermal ramp target cell having a peak temperature of 602 °C and the nail penetration target a peak temperature of 273 °C. The Thermal Ramp test has a higher peak temperature which leads to increased heat transfer to the neighboring cells and a greater likelihood that other cells within the battery pack fail.

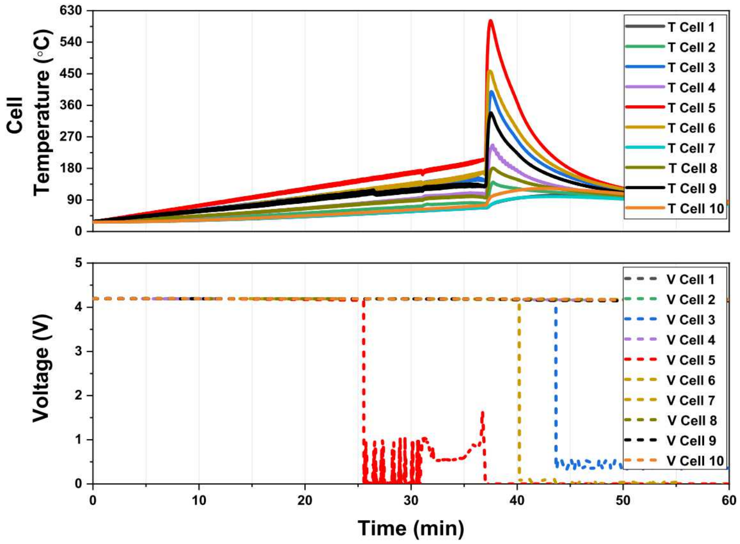


**Figure 10 Failure Propagation of a 10 cell LCO 18650 pack initiated through single cell thermal runaway.**

**Table 10 Numeric data of results shown in Figure 10.**

| **Test #2** | | | | |
|---|---|---|---|---|
| *Cell #* | *Propagation time (s)* | *Onset T (°C)* | *Max T (°C)* | *Max dT/dt (°C/min)* |
| 1 | N/A | N/A | 104 | 32 |
| 2 | N/A | N/A | 141 | 185 |
| 3 | 3 | 145 | 399 | 771 |
| 4 | N/A | N/A | 247 | 456 |
| **5** | **0** | **206** | **602** | **2253** |
| 6 | 0 | 165 | 457 | 1409 |
| 7 | N/A | N/A | 100 | 26 |
| 8 | N/A | N/A | 181 | 260 |
| 9 | N/A | N/A | 339 | 971 |
| 10 | N/A | N/A | 123 | 98 |

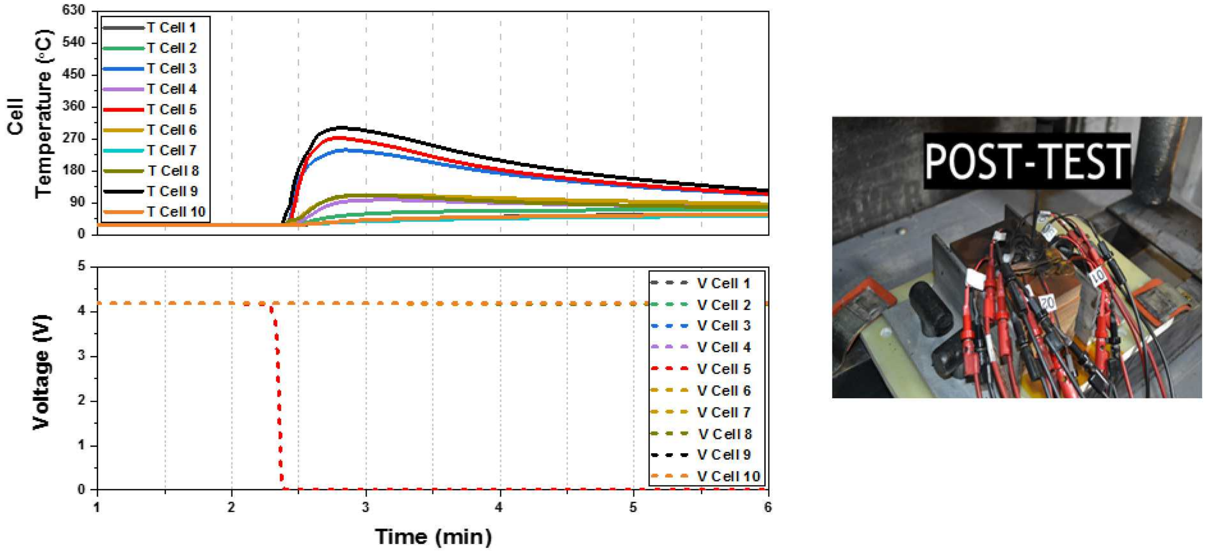


**Figure 11 Failure propagation test of a 10 cell LCO 18650 pack initiated through single cell nail penetration.**

**Table 11 Numeric data of results seen in Figure 11.**

| **Test #2** | | |
|---|---|---|
| *Cell #* | *Max T (°C)* | *Max dT/dt (°C/min)* |
| 1 | 58.7 | 28.5 |
| 2 | 70 | 99 |
| 3 | 239.2 | 1696.5 |
| 4 | 98.8 | 241.5 |
| **5** | **272.8** | **1603.5** |
| 6 | 112.5 | 327 |
| 7 | 55.3 | 24 |
| 8 | 111.7 | 297 |
| 9 | 301.1 | 1543.5 |
| 10 | 57.8 | 31.5 |

## 3.5. Comparing the effect of electrical connectivity to the effect of initiation method

The results presented in section 3.4 present the case where the single cell thermal runaway initiation method used presented the most significant impact to the results. Further work was performed on this method by exploring the effects using different electrical configuration. Parallel configurations have been shown previously [26] to lead to more severe failure propagation due to short circuit conditions created at the point of failure that force other cells to discharge. It is however conceivable that different test methods will respond differently.  Nail penetration creates an immediate internal short circuit within the cell, meanwhile a thermal ramp increases cell resistance until a shortcircuit occurs during thermal runaway.

Figures 12 and 13 show the results using nail penetration and thermal ramp initiation in 1S10P packs built with the 18650 LCO cells used in this study. These results do show some changes between tests; notably the propagation becoming more severe in each case. The nail penetration results showed a peak temperature of 1122 °C, which notably occurred on one of the exterior cells in the pack. Post test examination showed that the likely reason the entire pack wasn't consumed was due to the loss of electrical connection between cells as the interconnects could not sustain the high currents caused by the discharge.

Thermal ramp initiation led to an observed peak temperature of 1143 °C and was accompanied by a complete thermal runaway propagation that consumed the entire pack. In this case, the increase in severity of the thermal ramp test coupled with the impact of a parallel connection was able to drive all cells within the pack into thermal runaway. There remains some difference between the two packs, however, some evidence suggests that that they would exhibit similar results with more robust cell interconnects as might be used in high power applications. The primary support for this is the similar peak temperatures that were observed between the two packs.

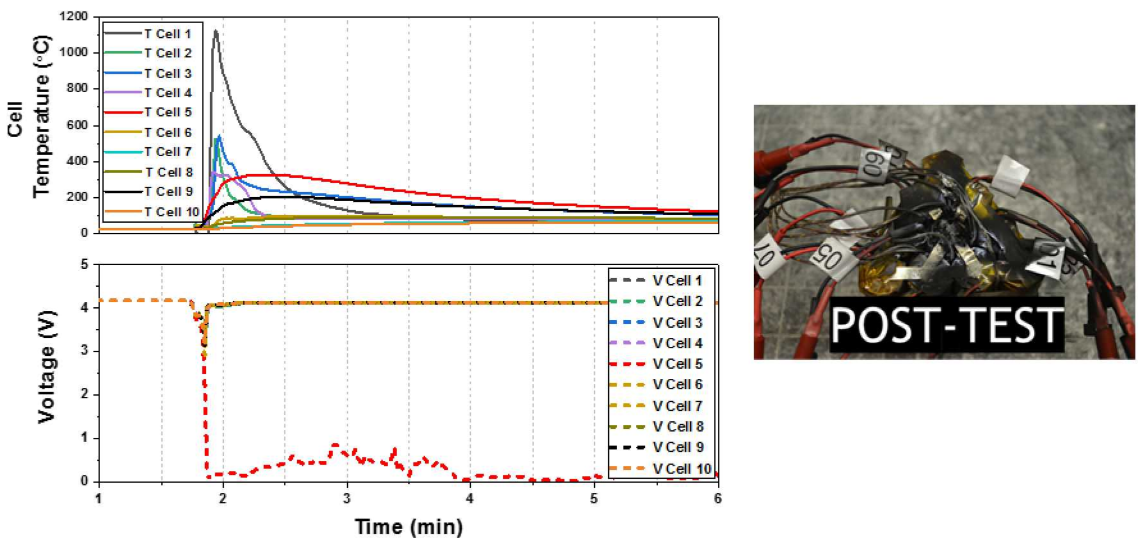


**Figure 12 10 cell 18650 LCO pack connected in a 1S10P configuration with failure initiation using a single cell nail penetration test**

**Table 12 Numeric data from results seen in Figure 12.**

| Test #2 |
| --- |

| *Cell #* | *Max T (°C)* | *Max dT/dt (°C/min)* |
|---|---|---|
| 1 | 1122.2 | 16833 |
| 2 | 521.8 | 6814.5 |
| 3 | 542.3 | 6334.5 |
| 4 | 342.5 | 4641 |
| **5** | **326.9** | **1734** |
| 6 | 100.7 | 513 |
| 7 | 68.5 | 49.5 |
| 8 | 90.1 | 220.5 |
| 9 | 206.3 | 793.5 |
| 10 | 65.7 | 46.5 |

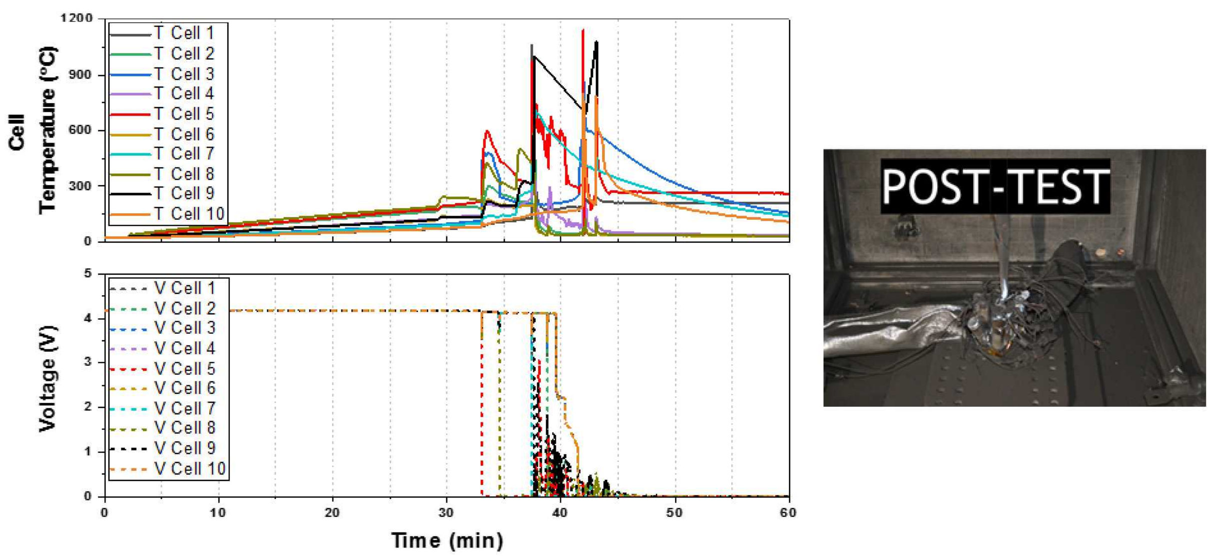


**Figure 13 10 cell 18650 LCO pack in 1S10P configuration with failure initiation due to single cell thermal ramp.**

**Table 13 Numeric data of results seen in Figure 13**

| **Test #2** | | |
|---|---|---|
| *Cell #* | *Max T (°C)* | *Max dT/dt (°C/min)* |
| 1 | 1064 | 11278 |
| 2 | 926 | 8574 |
| 3 | 897 | 5082 |
| 4 | 676 | 8603 |
| **5** | **1143** | **12441** |
| 6 | 231 | 822 |
| 7 | 708 | 1806 |
| 8 | 588 | 2148 |
| 9 | 1082 | 7820 |
| 10 | 802 | 9173 |

## 3.6. Comparing effect of initiation method to effect of energy density

The overall comparison of the three major pack configurations tested shows that a likely dominant factor in the propagating failure behavior is the energy density of the system. Further testing of this was performed by evaluating nail penetration and thermal ramp results in the highest energy density configuration, but reducing the total state of charge to 80% nominal state of charge prior to testing. This effectively creates a pack with reduced energy density, but still strong thermal contact between cells due to the stacking of the pouch cells.

Test results presented in Figures 14 and 15 show that even at the reduced total energy, both packs exhibited a fully propagated failure. However, some overall behaviors are different between the two tests. Thermal ramp initiation showed a peak temperature of 637 °C and all cells were consumed after 64 seconds. These results are virtually unchanged from the equivalent test at 100% SOC above. The test initiated with nail penetration saw a peak temperature of 506 °C and required 198 seconds to fully consume all cells in the test. So, while thermal runaway was still observed, there was an increase in time required by almost 5x.

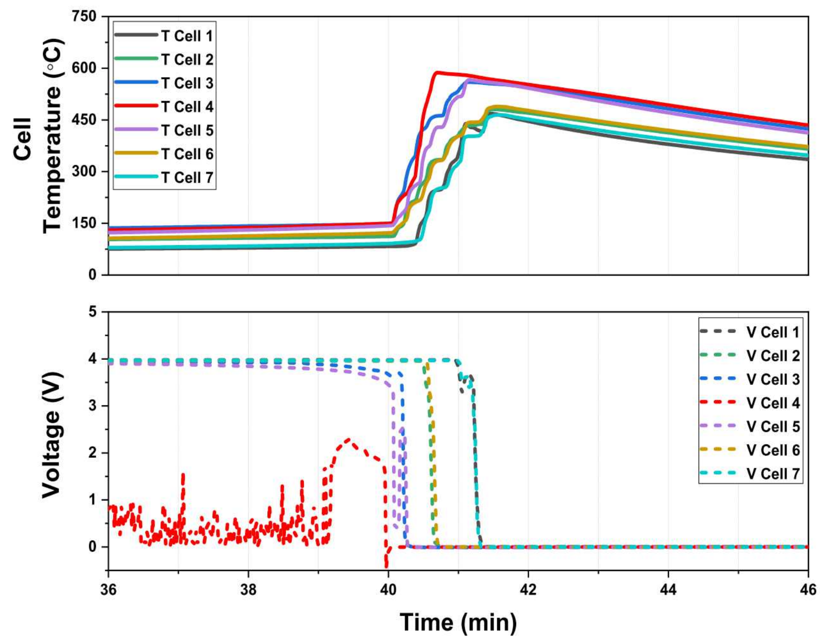


**Figure 14 5 Ah NMC pouch packs reduced to 80% nominal state of charge with propagating failure induced by single cell thermal ramp test.**

**Table 14 Numeric data from results shown in Figure 14**

| **Test #1** | | | | |
|---|---|---|---|---|
| *Cell-runaway order* | *Propagation time (s)* | *Onset T (°C)* | *Max T (°C)* | *Max dT/dt (°C/min)* |
| **4** | **0** | **150** | **637** | **2283** |
| 5 | 7 | 145 | 623 | 1540 |
| 3 | 14 | 151 | 621 | 1671 |
| 2 | 33 | 114 | 586 | 1540 |
| 6 | 36 | 124 | 576 | 1634 |
| 7 | 61 | 91 | 517 | 1639 |
| 1 | 64 | 106 | 483 | 1690 |

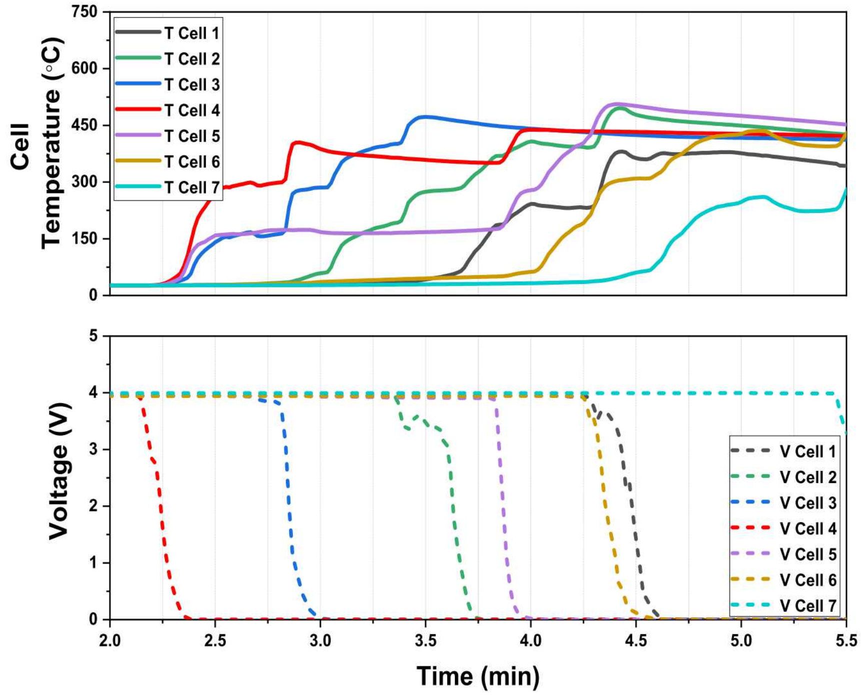


**Figure 15 5 Ah NMC pouch cell pack with failure initiated through single cell nail penetration.**

**Table 15 Numeric data of results shown in Figure 15.**

| **Test #1** | | | | |
|---|---|---|---|---|
| *Cell-runaway order* | *Propagation time (s)* | *Onset T (°C)* | *Max T (°C)* | *Max dT/dt (°C/min)* |
| **4** | **0** | **RT** | **438** | **1924** |
| 3 | 39 | 163 | 472 | 1674 |
| 2 | 73 | 193 | 495 | 1192 |
| 5 | 101 | 176 | 506 | 1169 |
| 6 | 126 | 192 | 490 | 1097 |
| 1 | 128 | 233 | 381 | 1658 |
| 7 | 198 | 228 | 379 | 1526 |

## 3.7. Use of fast localized heating as initiator

An initiation method that has been used in various laboratories is to use a small area heater at high power to create a localized hot spot and associated thermal runaway within a lithium ion battery. This “patch heater” method attempts to recreate the single cell thermal runaway characteristics of a thermal ramp test without significantly raising the temperature of the other cells in the pack. This test that can be easily performed by most testing laboratories, as it requires little in the way of specialized equipment (beyond that needed to safely perform battery abuse testing). This method was evaluated as part of this work and performed on the 10 cell 18650 LCO pack, as that showed the greatest differences between test methods. The patch heater was built in the lab and used to heat the target cell at a high rate until thermal runaway occurred.

Figure 16 and Table 16 show the results of this test. This method shows only the target cell going into thermal runaway, with a maximum observed temperature of 608 °C. (Note that a thermocouple failure was caused by the high heating rate of the patch heater leading to a false high temperature reading that can be observed in the graph). While some neighboring cells reach significantly high temperatures, they do not heat in the bulk long enough to go into thermal runaway. Although this test does not provide the zero heating condition observed with nail penetration, it does provide a propagating failure result that is closer to that condition than the traditional thermal ramp test. This is most applicable to cylindrical cells, where it is more feasible to limit the patch heater’s impact on neighboring cells.

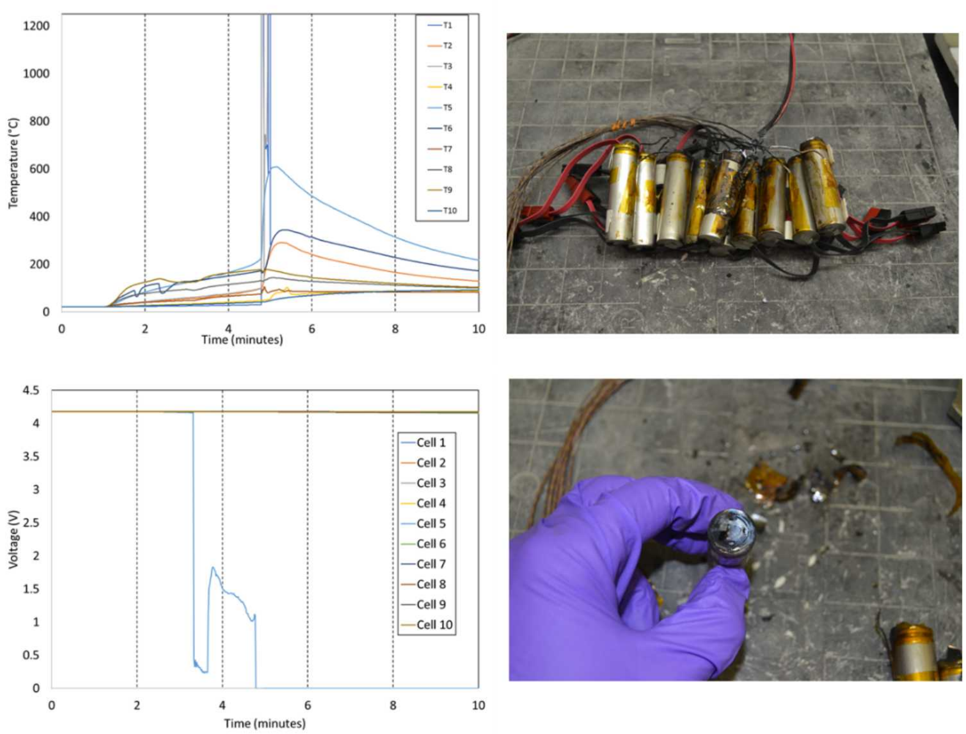


**Figure 16 10 cell LCO 18650 pack initiated through the use of fast heating of a small area (“patch”) heater on a single cell.**

**Table 16 Numeric data of results shown in Figure 16**

| **Test #1** | | |
|---|---|---|
| *Cell #* | *Max T (°C)* | *Max dT/dt (°C/min)* |
| 1 | ND | ND |
| 2 | 291.6 | 1158 |
| 3 | 542.3 | 6334.5 |
| 4 | 102.7 | 294 |
| **5** | **608.3** | **5892** |
| 6 | 344.3 | 906 |
| 7 | 105.9 | 978 |
| 8 | 143.4 | 114 |
| 9 | 178 | 228 |
| 10 | 92.4 | 54 |

# 4. CONCLUSIONS AND PROPOSED GUIDANCE FOR PROPAGATION TESTING

This work presents a detailed study on the use of conventional abuse test methods and their impact on propagation test results. Overall, this work has found that while there is some impact from the selection of initiation method, it is not necessarily the strongest factor in determining the likelihood and severity of battery failure propagation. Notably, the energy density of the battery pack plays a significant role in the failure propagation behavior, with high energy density packs exhibiting a higher likelihood of leading to a propagating failure regardless of the initiation method used. Other system design elements, such as electrical connectivity and packing efficiency of the cells within a system can have a strong impact. on failure propagation test results. These can both create or limit paths for heat transfer and conduction between cells and have a strong impact on thermal runaway propagation.

The strongest impact of initiation method was in packs that had some resistance to propagation in their default configuration. , Results show that methods that add significant amounts of energy to the target cell prior to failure had noticeable different behaviors from methods that limited the additional energy into the cell. This observation indicates that that care must be taken in the selection of an initiation method when packs are being built with some inherent resistance in mind. It should also be considered if the objective of the research is to probe the "worst case scenario" or "worst credible event", further discussed in section 4.1. The test objectives must be accounted for when selecting an initiation method.

Unfortunately, this work does not present a universal initiation method. The goals of a test program and test limitations of both the test unit and the facility performing testing must all be considered. This work does however, present lessons learned that can provide guidelines when performing failure propagation testing on lithium ion battery systems. This work presents a set of proposed guidelines and best practices for selecting a battery failure initiation method. Ultimately, this hopes to provide an overall benefit to public safety as it allows us to better understand how susceptible large battery systems might be to a single cell battery failure propagating thermal runaway events to the rest of the system.

## 4.1. Proposed guidelines and best practices for initiation method selection

### *4.1.1. Establish goals of testing program during test planning*

Safety testing of batteries can generally be thought of as pursuing one of two goals: understanding the "worst-case scenario" or understanding the "worst credible event." Testing to understand the worst-case scenario means pursuing the most severe possible consequence of a battery failure, regardless of the likelihood of its initiation. This level of testing can be useful as it establishes the most severe consequences of failure of the battery system in question. Much of battery abuse testing ultimately falls in this category. However, it does not necessarily establish true risk, as the methods used to reach that condition may be very unlikely.

Testing for a "worst credible event" means making an effort, prior to testing, in discerning what failure scenarios can credibly occur during the lifecycle of the system. This allows a better idea of the safety risk to be established with the introduction of potential margins of error. This ultimately relies on a judgement from Subject Matter Experts on what events are credible and can lead to catastrophic events if that judgement is incorrect.

### 4.1.2. Single cell testing to establish a reliable runaway condition and understand the results of selected method

Because primary goal of failure propagation testing is to determine the system response to a single cell thermal runaway, it is imperative that any initiation method chosen can reliably initiate a thermal runaway in a single cell. It should be established prior to testing that any initiation method being used can reliably initiate a thermal runaway within a single cell from the battery in question. Selection can be determined by performing single cell abuse testing with candidate initiation methods. Desired information may also be available from other organizations or in the public record. It should be noted as well that cells many cells have inherent safety devices that interfere with some abuse tests. This should be determined early in the test plan development.

### 4.1.3. Minimize impact to the system beyond the target cell or cells

It is a best practice to select a method that minimizes impact to the system beyond the targeted cell. This minimizes the likelihood that the results will be impacted by increased energy input into the pack. The "energy input totals", mentioned earlier in the report, can be used as a guideline. Ultimately, data has shown that nail penetration and small area heaters are able to minimize the impact to neighboring cells.

### 4.1.4. Consider physical realities of the test article and facility performing the work

Ultimately, a single cell within the pack needs to be targeted by type of propagation failure test, and there may be physical realities of the pack itself or the facility performing the test that precludes performing certain tests. During the planning phase of any test program, it should be quickly identified what single cell thermal runaway tests can be easily performed by the testing organization while also considering the constraints of the device being tested.

## REFERENCES


1. Musk, E., *Model S Fire*, in *Tesla Blog*. 2013.
2. Voelcker, J. *Chrysler Yanks Plug-In Hybrid Test Fleet Off Roads, Will Replace Batteries*. Green Car Reports 2012 [cited 2014 8-7-2014]; Available from: http://www.greencarreports.com/news/1079368_chrysler-yanks-plug-in-hybrid-test-fleet-off-roads-will-replace-batteries.
3. Lowy, J. *Overcharging batteries eyed in Boeing 787 mishaps*. Phys.org 2013 [cited 2014 8-7-2014].
4. Arbizzani, C., G. Gabrielli, and M. Mastragostino, *Thermal stability and flammability of electrolytes for lithium-ion batteries*. Journal of Power Sources, 2011. **196**(10): p. 4801-4805.
5. Bandhauer, T.M., S. Garimella, and T.F. Fuller, *A Critical Review of Thermal Issues in Lithium-Ion Batteries*. Journal of The Electrochemical Society, 2011. **158**(3): p. R1-R25.
6. Campion, C.L., W.T. Li, and B.L. Lucht, *Thermal decomposition of LiPF6-based electrolytes for lithium-ion batteries*. Journal of The Electrochemical Society, 2005. **152**(12): p. A2327-A2334.
7. Dahn, J.R. and G.M. Ehrlich, *Lithium-Ion Batteries*, in *Linden's Handbook of Batteries*, T.B. Reddy, Editor. 2011, McGraw Hill: New York. p. 26.1-79.
8. Doughty, D.H., et al., *Lithium battery thermal models*. Journal of Power Sources, 2002. **110**(2): p. 357-363.
9. Doughty, D.H., et al., *Effects of additives on thermal stability of Li ion cells*. Journal of Power Sources, 2005. **146**(1-2): p. 116-120.
10. Fei, R., T. Cox, and W. Hsin, *Thermal runaway risk evaluation of Li-ion cells using a pinch-torsion test*. Journal of Power Sources, 2014. **249**: p. 156-162.
11. Jeevarajan, J.A., et al., *Performance characterization and safety testing of lithium-ion cells and battery for space flight applications*. Lithium Batteries, Proceedings, ed. S. Surampudi, et al. Vol. 99. 2000, Pennington: Electrochemical Society Inc. 694-705.
12. Jhu, C.Y., et al., *Self-reactive rating of thermal runaway hazards on 18650 lithium-ion batteries*. Journal of Thermal Analysis and Calorimetry, 2011. **106**(1): p. 159-163.
13. Kim, G.-H., A. Pesaran, and R. Spotnitz, *A three-dimensional thermal abuse model for lithium-ion cells*. Journal of Power Sources, 2007. **170**(2): p. 476-489.
14. Roth, E.P., *Abuse response of 18650 Li-Ion cells with different cathodes using EC:EMC/LiPF6 and EC:PC:DMC/LiPF6 electrolytes*. Battery Safety and Abuse Tolerance at the 212th ECS Meeting, 2008: p. 19-4141.
15. Roth, E.P., et al., *Advanced technology development program for lithium-ion batteries: thermal abuse performance of 18650 Li-ion cells. SAND2004-0584*. 2004, Sandia National Laboratories: Albuquerque, NM.
16. Spotnitz, R.M., et al., *Simulation of abuse tolerance of lithium-ion battery packs*. Journal of Power Sources, 2007. **163**(2): p. 1080-1086.
17. Offer, G.J., et al., *Module design and fault diagnosis in electric vehicle batteries*. Journal of Power Sources, 2012. **206**(0): p. 383-392.
18. Friel, D.D., *Battery Design*, in *Linden's Handbook of Batteries*, T.B. Reddy, Editor. 2011, McGraw Hill: New York. p. 5.1-5.23.
19. Sun, H., et al., *Three-dimensional thermal modeling of a lithium-ion battery pack*. Journal of Power Sources, 2012. **206**(0): p. 349-356.
20. Kim, G.-H., et al., *Fail-safe design for large capacity lithium-ion battery systems*. Journal of Power Sources, 2012. **210**(0): p. 243-253.
21. Lu, L., et al., *A review on the key issues for lithium-ion battery management in electric vehicles*. Journal of Power Sources, 2013. **226**(0): p. 272-288.

22. Troxler, Y., et al., *The effect of thermal gradients on the performance of lithium-ion batteries.* Journal of Power Sources, 2014. **247**(0): p. 1018-1025.
23. Wu, B., et al., *Coupled thermal–electrochemical modelling of uneven heat generation in lithium-ion battery packs.* Journal of Power Sources, 2013. **243**(0): p. 544-554.
24. Wu, M.S., et al., *Correlation between electrochemical characteristics and thermal stability of advanced lithium-ion batteries in abuse tests - short-circuit tests.* Electrochimica Acta, 2004. **49**(11): p. 1803-1812.
25. Orendorff, C., J. Lamb, and L.A.M. Steele, *SNL Abuse Testing Manual.* 2017, Sandia National Laboratories: Albuquerque, NM.
26. Lamb, J., et al., *Failure propagation in multi-cell lithium ion batteries.* Journal of Power Sources, 2015. **283**: p. 517-523.

# DISTRIBUTION

**Email—External**

| Name | Company Email Address | Company Name |
|---|---|---|
| Steve Summers | | US Department of Transportation |

**Email—Internal**

| Name | Org. | Sandia Email Address |
|---|---|---|
| Christopher Orendorff | 2540 | |
| Kyle Fenton | 2546 | |
| Loraine Torres-Castro | | |
| June Stanley | | |
| Technical Library | 01177 | libref@sandia.gov |

This page left blank

This page left blank

Sandia National Laboratories

Sandia National Laboratories is a multimission laboratory managed and operated by National Technology & Engineering Solutions of Sandia LLC, a wholly owned subsidiary of Honeywell International Inc. for the U.S. Department of Energy's National Nuclear Security Administration under contract DE-NA0003525.